UNLV | University Libraries
University of Nevada, Las Vegas

Chemistry and Biochemistry Faculty Publications

Chemistry and Biochemistry

10-1998

Auger Resonance Decay Process in Ar 2p Shell Excitation and Ionization

Y. Lu
Behlen Laboratory of Physics

Wayne C. Stolte
University of Nevada, Las Vegas, wcstolte@lbl.gov

J.A. R. Samson
Behlen Laboratory of Physics

Follow this and additional works at: https://digitalscholarship.unlv.edu/chem_fac_articles

 Part of the Analytical Chemistry Commons, Atomic, Molecular and Optical Physics Commons, Biological and Chemical Physics Commons, and the Physical Chemistry Commons

Repository Citation

Lu, Y., Stolte, W. C., Samson, J. R. (1998). Auger Resonance Decay Process in Ar 2p Shell Excitation and Ionization. *Physical Review A, 58*(4), 2828-2833.
https://digitalscholarship.unlv.edu/chem_fac_articles/36

This Article is protected by copyright and/or related rights. It has been brought to you by Digital Scholarship@UNLV with permission from the rights-holder(s). You are free to use this Article in any way that is permitted by the copyright and related rights legislation that applies to your use. For other uses you need to obtain permission from the rights-holder(s) directly, unless additional rights are indicated by a Creative Commons license in the record and/or on the work itself.

This Article has been accepted for inclusion in Chemistry and Biochemistry Faculty Publications by an authorized administrator of Digital Scholarship@UNLV. For more information, please contact digitalscholarship@unlv.edu.

Auger-resonance-decay process in Ar $2p$-shell excitation and ionization

Y. Lu, W. C. Stolte,* and James A. R. Samson
Behlen Laboratory of Physics, University of Nebraska–Lincoln, Lincoln, Nebraska 68588-0111
(Received 20 March 1998)

The production and subsequent autoionization of the $Ar^+(^1D_2)6d'$ satellite state that is formed either by shake-up or recapture during the Auger decay of a $2p$ vacancy in Ar has been studied by photoelectron spectroscopy in the energy region from 243 to 256 eV. The creation of near zero energy electrons below and immediately above the Ar $2p$ ionization threshold is discussed. Some ambiguous points in previous studies are clarified. [S1050-2947(98)12609-4]

PACS number(s): 32.80.Dz, 32.80.Fb, 32.80.Hd

I. INTRODUCTION

When resonant excitation of an inner-shell electron in an atom results in an Auger decay there is a probability that the out-going Auger electron will interact with the photoexcited electron. The two electrons can exchange energy resulting in unexpected final states of the excited ion. This process is usually described as a shake-up or shake-down process [1–7]. A similar Auger or photoelectron interaction occurs when the atom is photoionized at or just above the inner-shell ionization thresholds. In this case the released photoelectron either can be captured into a discrete level of the ion or can escape with reduced kinetic energy. This process is called a postcollision interaction (PCI) [8–11]. However, in general the excitation and decay cannot be treated as separate events [12]. For example, photionization of an Ar $2p$ electron near threshold or photoexcitation at a specific $2p$-nd resonance can produce any of the following final states:

$$\mathrm{Ar}+\gamma\rightarrow Ar^{+}{}^{*}3p^{-2}(^3P,^1D,^1S)md+e_A \qquad (1)$$

$$\rightarrow \mathrm{Ar}^{+}{}^{*}3s^{-1}3p^{-1}(^1P,^3P)md+e_A, \qquad (2)$$

where e_A represents the Auger electron and m can be either greater or less than n. If the $Ar^{+}{}^{*}$ excited final states lie above the threshold for double ionization (see Fig. 1) autoionization can occur through a valence multiplet decay [13,14], as shown in the example below:

$$\mathrm{Ar}^{+}{}^{*}3p^{-2}(^1D)md'\rightarrow \mathrm{Ar}^{2+}3p^{-2}(^3P)+e_{auto}, \quad m\geqslant 6 \qquad (3)$$

where e_{auto} represents the electron produced by autoionization. Measurements of the kinetic energies of these electrons identify the Auger final state and hence the value of m. The production of excited ionic states through Auger decay and the knowledge that further decay is possible through a valence multiplet transition are very important in the interpretation of multiple ionization and photoelectron spectra [15–17].

Studies of threshold electrons by several groups [18–22] have revealed that near zero energy electrons are produced in the decay of all $\mathrm{Ar}2p^{-1}ns,nd$ resonances. Heimann *et al.* [18] interpreted their results on the basis of shake-off theory. But recent calculations predicted that shake-off was very unlikely [6]. Hayaishi *et al.* [19] proposed a two-step autoionization model in order to explain the increased production of zero energy electrons at the $2p^{-1}4d$ and $5d$ resonances. This model required the initial excited states to experience shake-up into final states lying just above a double ionization threshold, see Eqs. (2) and (3). Subsequent autoionization of these states could then occur through a valence multiplet Auger decay producing low-energy electrons. However, only the $(^1D)6d'$ final state appears to be a suitable candidate for this proposal (see Fig. 1). The binding energy for this state has been reported to be in the range from 43.42 to 43.44 eV, whereas the $(^1S)5d''$ state lies below the (^1D) double ionization threshold [3,23–28]. If the production of zero energy electrons by shake-off is ruled out then the question arises ''can shake-up or shake-down into the $(^1D)6d'$ level occur at all $2p^{-1}ns,nd$ resonances?''

In the present work we report on our studies of the probability for producing the $(^1D)6d'$ satellite state at photon energies coincident with the resonances and at energies above the $L_{2,3}$ ionization thresholds.

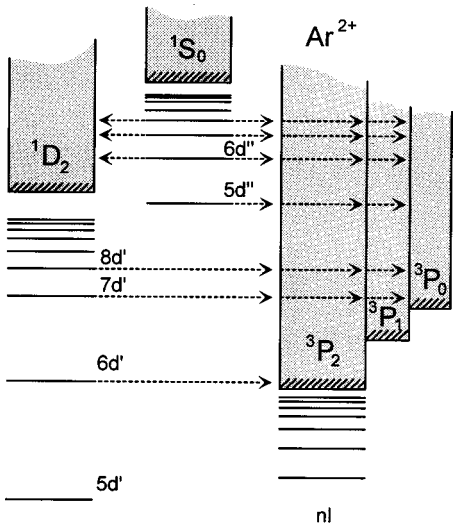

FIG. 1. Energy-level diagram of the $Ar^{2+}(^3P,^1D,^1S)$ continua. The discrete Rydberg states leading up to double ionization represent the $Ar^{+}{}^{*}$ satellite states. The possible autoionization pathways are indicated by arrows.

*Present address: Department of Chemistry, University of Nevada, Las Vegas, NV 89154.

 © 1998 The American Physical Society

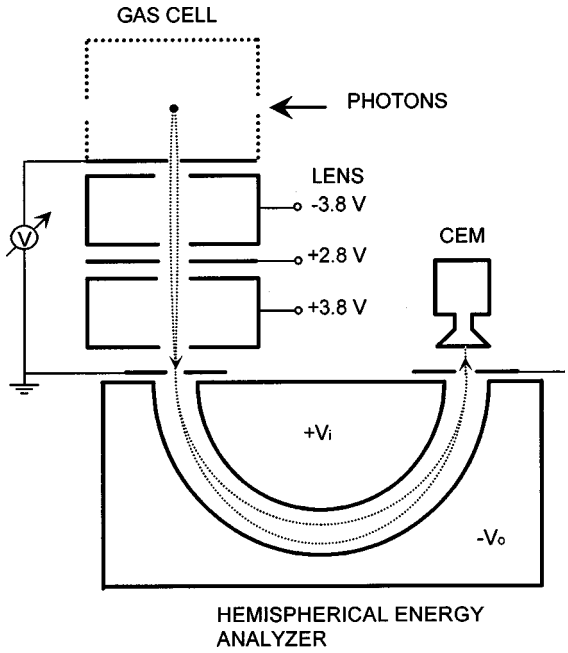

FIG. 2. Experimental arrangement of the hemispherical electron-energy analyzer, electron lens, gas cell, and channel-electron detector. A variable voltage was applied to the gas cell to provide a constant 5-eV pass energy for the energy analyzer.

II. EXPERIMENT

An electron energy analyzer was used in conjunction with synchrotron radiation to study the low-energy electron spectrum between 0 and 6 eV produced by the Auger decay of the $2p^{-1}$ vacancy in Ar. The experiment was performed at the Advanced Light Source in Berkeley, California, on the bending magnet beamline 6.3.2. The synchrotron radiation was dispersed by a plane grating (600 lines/mm) grazing incidence monochromator. The photon band pass used was varied for different measurements but was typically in the range of 0.1 to 0.5 eV. The energy scale of the monochromator was calibrated using the Ar $2p$-$4s$ absorption line at 244.39 eV$\pm$0.01 eV [29]. The electron energies were analyzed with a 180° spherical energy analyzer with a mean radius of 5 cm. The analyzer was set for a pass energy of 5 eV, which gave a resolution of about 50 meV. To obtain an accurate energy calibration, the binding energy of the Ar$(^1D)6d'$ state was measured in a separate experiment. This made use of the high-resolution electron-energy analyzer Scienta in conjunction with the PGM undulator beamline at the Synchrotron Radiation Center in Wisconsin. We measured the binding energy to be 43.412 eV$\pm$0.005 eV. Subtracting this value from the known $^3P_2$ double ionization threshold at 43.3893 eV [30] gives an energy value of 23 meV for the electrons produced by autoionization of the $(^1D)6d'$ state into the $^3P_2$ continuum.

The electrons were detected at right angles to the photon beam and to the radiation polarization vector. The ionization region was surrounded by mesh in order to reduce the background of scattered electrons. The arrangement of gas cell, electron lens, and analyzer is shown in Fig. 2.

III. RESULTS

Figure 3 shows the low-energy electron spectra obtained from the decay of the resonantly excited $2p^{-1}ns,nd$ states.

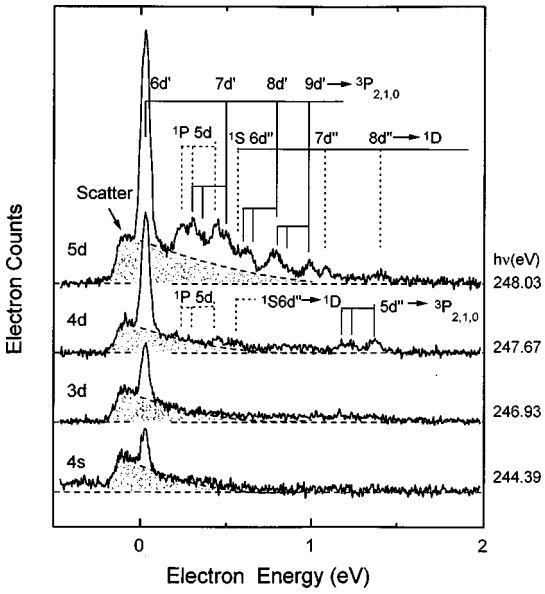

FIG. 3. Low-energy electron spectra produced in the Auger decay of the $2p^{-1}ns,nd$ resonances via autoionization of the shake-up states. The broad background peaks near the zero energy region were caused by scattered electrons.

We see that each state experiences shake-up into the $3s^2 3p^4(^1D)6d'$ final state, which then autoionizes into the $^3P_2$ continuum, producing a 23-meV electron. The zero of the energy scale is based on this value. The 50-meV half-width of the $6d'$ line and of the remaining structure shown in Fig. 3 reflects the resolution of the energy analyzer only and does not depend on the resolution of the incident radiation, which was about 0.5 eV. This is evidence that these lines all originate through autoionization. The data taken at the $4d$ and $5d$ resonances also show structure due to shake-up into higher n values. However, there may be some contamination from direct excitation into the $6d'$ and $7d'$ resonances because of the poor photon resolution. There is a broad scattered electron peak that has a maximum below the zero energy position and a tail on the higher-energy side. These scattered electrons are caused by the Auger electrons hitting the edge of the exit aperture of the ionization cell. The field distribution within the ionization cell, which depends on the geometry of the ionization region and its exit aperture, will push any zero-kinetic-energy electrons produced there through the analyzer at a lower voltage than that for the zero-kinetic-energy electrons produced in the ionization region. The zero-kinetic-energy scattered electrons will then appear at a position below the zero position of the spectrum. If the low-energy electrons observed at the Ar $2p$ resonances were caused by shake-off, this would produce electrons with a continuous energy distribution starting at zero. But because these electrons would be produced in the ionization region they should appear exactly at the zero position of the spectrum. Thus, it is unlikely that the background continuum observed in the present spectrum is caused by shake-off.

The electron-energy spectra taken at photon energies exactly at the L_3 and L_2 thresholds are shown in Fig. 4. At these thresholds we would expect to see, respectively, the zero energy $2p_{3/2}$ and $2p_{1/2}$ photoelectron peaks. Instead, because of the PCI effect, the zero energy electrons are cap-

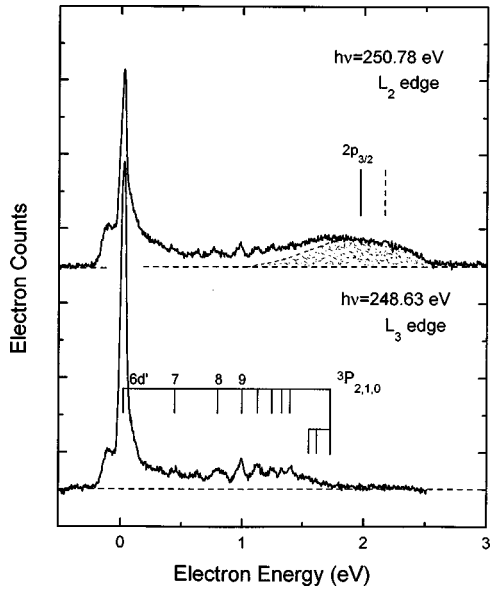

FIG. 4. Low-energy electron spectra produced in the Auger decay of the $2p^{-1}$ hole at the $L_{2,3}$ thresholds. Recapture of the photoelectrons into the $(^1D)nd'$ states and their subsequent autoionization can be seen in both spectra. The $2p_{3/2}$ photoelectron peak can be seen in the L_2 spectrum retarded by about 0.2 eV from its expected peak position (vertical dashed line).

tured into the various discrete levels of Ar^+. A certain fraction are captured into the $(^1D)nd'$ levels. At the L_3 threshold we see autoionization of the nd' levels into the $^3P_{0,1,2}$ continuum ($n \geq 6$) terminating at 1.74 eV for $n=\infty$. Although direct excitation of some of these lines will contribute to the spectrum we note that in our previous work, using a photon energy of 248.8 eV, the entire $(^1D)nd'$ series was also populated from $n=6$ to infinity [17]. In this case direct excitation was not possible. At the L_2 threshold a similar spectrum occurs because of the capture of the $2p_{1/2}$ photoelectrons. However, a high percentage of the energetic $2p_{3/2}$ photoelectrons escape giving the broad peak near 2 eV.

In Fig. 5 both the $2p_{1/2}$ and $2p_{3/2}$ photoelectrons appear.

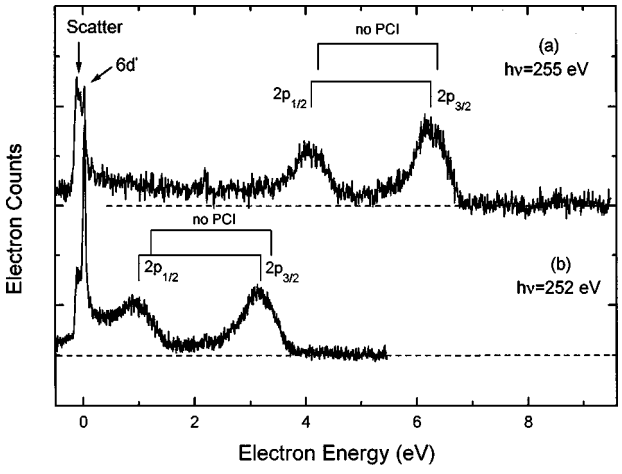

FIG. 5. Photoelectron energy spectra observed above the Ar $2p$ ionization threshold. The peaks are retarded by 0.10 to 0.22 eV from their expected positions due to the PCI effect. Note that final shake-up into the $(^1D)6d'$ state still persists.

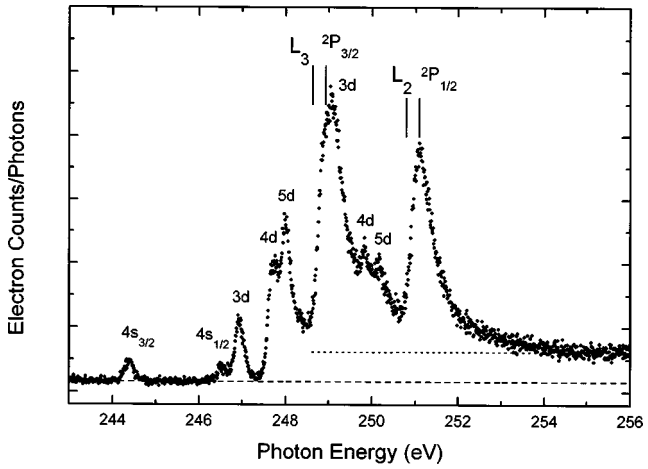

FIG. 6. Low-energy (23-meV) electron production measured as a function of the incident photon energy. Below the L_3 edge the data represent the probability for production of the $(^1D)6d'$ state through shake-up. Above the L_3 edge the data represent a combination of sources, namely, recapture of photoelectrons into the $(^1D)6d'$ state and retardation of the photoelectrons.

The peaks have broadened line shapes, in excess of that caused by the photon-energy resolution, and retarded peak positions caused by the PCI effect [31]. A small fraction of these energetic electrons are still captured into the $(^1D)6d'$ level, as shown in the figure.

In order to determine the probability for producing the $(^1D)6d'$ state, the energy analyzer was set to collect the electrons that appeared at the position of the $6d'$ peak, which included the underlying scattered electrons. Then the photon energy was scanned between 243 and 256 eV with a resolution of 200 meV. The results are shown in Fig. 6. This spectrum represents the relative probability for producing the $(^1D)6d'$ final state as a function of the incident photon energy, but it is uncorrected for the scattered electron background shown in Figs. 3–5. The contribution to the peaks caused by scattered electrons can be estimated from these figures. For example, from Fig. 3 the scattered signal accounted for 40%, 30%, 16%, and 14% of the intensity of the $4s$, $3d$, $4d$, and $5d$ peaks, respectively. Applying these corrections to the resonances in Fig. 6, we obtain the relative shake-up probabilities. These values were normalized to the calculated values given by Meyer *et al.* [5] for the $4d$ resonances. Clearly the $4d$ and $5d$ lines are not completely resolved in Fig. 6, thus the results are approximate. The results are tabulated in Table I and compared with the calculated and experimental values given by Meyer *et al.* [5] and by Mursu *et al.* [3]. Theory predicts a negligible amount of shake-up from the $2p^{-1}4s$ and $3d$ initial states into the $6d'$ final state, whereas our present results indicate otherwise. The ratio of the $4d$ to $5d$ line intensities are in qualitative agreement with the calculated values given by Meyer *et al.*

Above the L_3 threshold the origin of the spectrum is more complicated because of the PCI effect. For photon energies several electron volts above the threshold all photoelectrons are retarded by varying amounts, even to the point of being reduced to 0 eV or captured into a discrete level of Ar^+. In Fig. 5(b) the $2p_{1/2}$ photoelectron should have a discrete energy of 1.22 eV. Instead, it peaks at 1 eV but has a continu-

TABLE I. Approximate shake-up probabilities from core excited states $2p^{-1}nd$ into the $3s^2 3p^4(^1D)6d'$ state.

Initial excited states	Relative shake-up probabilities				
	Present data	Meyer *et al.* [5]		Mursu *et al.* [3]	
	Expt.	Calc.	Expt.	Calc.	Expt.
$2p^5 4s$	2.7				
$3d$	10	0.004		0.0	1.7
$4d$	24	24	32	34.5	14.2
$5d$	~ 34[a]	32			
$6d$		13			

[a]Estimated value.

ous range of energies down to 0 eV, including capture into the $6d'$ final state. Thus, in Fig. 6, above the L_3 threshold, the spectrum consists of three electron groups produced by (i) retardation, consisting of all electrons that are retarded to yield energies of 23 meV $\pm$ 25 meV; (ii) capture, consisting only of 23-meV electrons produced by electron capture into the $6d'$ state, followed by autoionization of that state; and (iii) excitation of the $2p_{1/2}^{-1}nd$ resonances, consisting of 23-meV electrons produced by shake-up into the $6d'$ final state and subsequent autoionization.

There is a strong similarity between the spectrum shown in Fig. 6 and the ''threshold'' photoelectron spectra observed by previous investigators [18–21]. Comparing our results below with the L_3 threshold with that of Avaldi *et al.* [20] we note that the ratio of their intensities for $3d{:}4d{:}5d$ lines are in excellent agreement with the present data. Above the L_3 threshold the intensities of their photoelectron peaks relative to the nd resonances are much larger. This can be explained on the basis that threshold energy analyzers have a higher collection efficiency for zero energy electrons than for 23-meV electrons. The base line shown in Fig. 6 represents the level of the background electrons caused by the double photoionization of the valence shell electrons. The magnitude of the scattered electron background produced by Auger electrons striking the exit aperture of the ionization cells varies depending on the intensity of the Auger electron signal. Above the L_3 edge we assume that this background is approximately constant and is represented by the electron signal at 256 eV.

We now wish to determine the contribution of electron capture to the production of the $(^1D)6d'$ state at energies above the L_3 edge. To a first approximation we assume that the production of the $6d'$ final state by electron capture is proportional to the total recapture probability. In our recent PCI studies of Ar [16] we obtained an experimental recapture probability curve in good agreement with the calculated results of Tulkkii *et al.* [11], which explained the production of Ar^+ above the $L_{2,3}$ thresholds. We also found that a constant fraction of the captured electrons were reemitted. The reemitted electrons were of course a consequence of capture into highly excited states, primarily $(^1D)nd'$ states with $n \geqslant 6$. Thus, normalizing the recapture probability curve to the data in Fig. 7 just at the L_3 and L_2 edges gives the continuation of the probabilities for producing the $6d'$ state above the thresholds. This is shown by the dotted curves in Fig. 7. The solid curve is explained in the discussion below.

The difference between the dotted curves and the experimental points (excluding the resonances) represents the contribution by retardation to the production of the 23-meV photoelectron peaks. To predict the line shapes of these peaks we followed the procedure described by Heimann *et al.* [18], who applied Niehaus's semiclassical model [9] to calculate their threshold photoelectron line shapes. The parameters we used were the linewidth of the Ar $2p$ level, $\Gamma = 120$ meV, and the photoelectron energy (23 meV). The results were convoluted with a Gaussian bandpass function with a half-width of 200 meV. This half-width represents the photon bandpass used for this experiment. The line shape obtained from this calculation as a function of the excess energy above the ionization threshold is shown in Fig. 8. The same result was obtained for a zero energy photoelectron. The shift in the peak position was 320 meV and the half-width of the line was 500 meV. This is in agreement with the calculations of Armen and Levin [32], who used a quantum-mechanical hydrogenic model. The solid line results shown in Fig. 8 represent the relative probability for producing 23-meV electrons through retardation. We added this result to the recapture curve at the L_3 threshold, adjusting the peak height to normalize the sum to the experimental peak value. The results are shown by the solid line in Fig. 7. This procedure was repeated at the L_2 threshold. We see that without con-

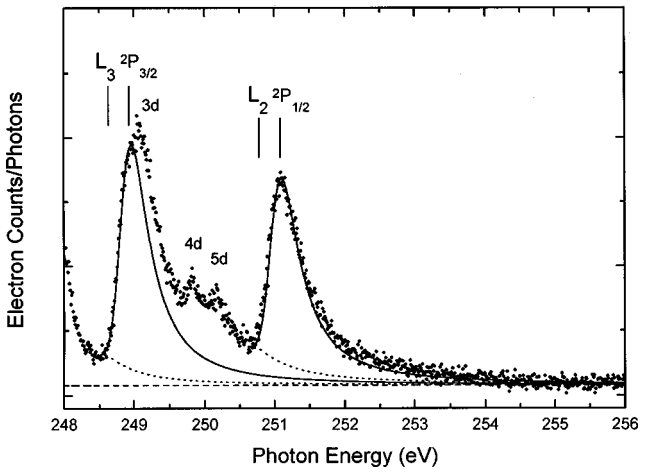

FIG. 7. Low-energy (23-meV) electron production above the L_3 edge. The contribution from electron recapture into the $(^1D)6d'$ state is given by the dotted curves. The solid curve represents the sum of the electron recapture and retardation curves (see Fig. 8).

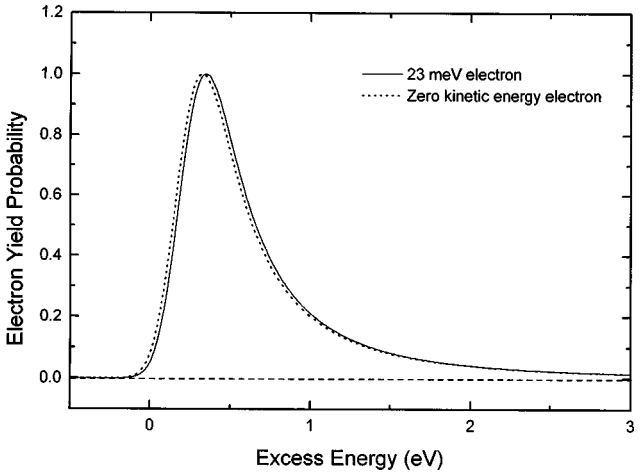

FIG. 8. Calculated electron yield probability for producing zero and 23-meV electrons as a function of the excess energy above the ionization threshold. The semiclassical model of Niehaus was used and convoluted with a Gaussian function (200-meV photon resolution).

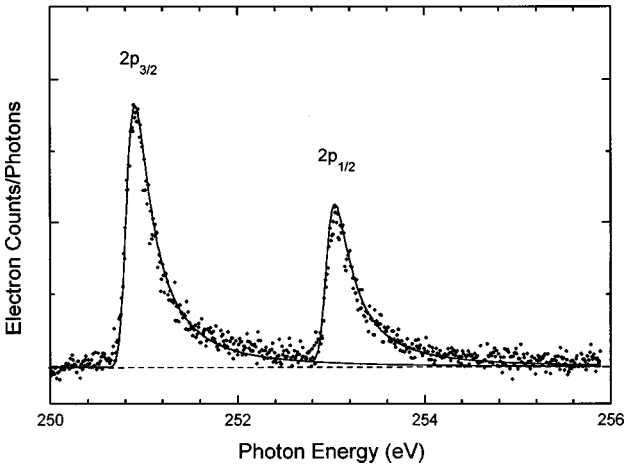

FIG. 9. Constant-energy (2-eV) photoelectron spectrum measured as a function of the photon energy. The solid curve represents the predicted electron yield using the Niehaus model convoluted with a Gaussian function (100-meV photon resolution).

sidering the contribution from the recapture curves the calculated PCI line shapes would not reproduce the experimental results at the $L_{2,3}$ edges. Thomas and co-workers [21] have discussed the need to convolute the semiclassical line shapes with additional Lorentzian broadening in order to obtain a better fit with their experimental data. Armen and Levin [32] argue that the agreement between their quantum model and the semiclassical model indicates that extra convolution is unjustified, and if so, then what causes the difference between theory and experiment at the threshold? We submit that the cause is the production of near zero energy electrons created by the capture of the excited and ejected photoelectrons (below and above the thresholds, respectively) into the $(^1D)6d'$ state and their subsequent decay by autoionization producing 23-meV electrons. This extra source of near zero energy electrons must be continuous across a threshold and then must decrease in a manner similar to that of the recapture probability curve [11]. If no suitable bound states exist to provide low-energy autoionized electrons then this problem does not exist. To illustrate this we have measured the constant energy spectrum for 2-eV electrons, which occurs well above the $L_{2,3}$ thresholds, as shown in Fig. 9. The photon resolution in this case was 100 meV and the electron resolution was 40 meV. Applying the Niehaus model again and simply renormalizing the curves to the photoelectron peak heights, we see there is an excellent fit to the experimental data.

ACKNOWLEDGMENT

This research was supported by the National Science Foundation under Grant No. PHY-9317934.

[1] H. Aksela, S. Aksela, H. Pulkkinen, G. M. Bancroft, and K. H. Tan, Phys. Rev. A **37**, 1798 (1988).
[2] H. Aksela, S. Aksela, A. Mäntykenttä, J. Tulkki, and Y. Furusawa, Phys. Scr. **T41**, 113 (1992).
[3] J. Mursu, H. Aksela, O.-P. Sairanen, A. Kivimäki, E. Nõmmiste, A. Ausmees, S. Svensson, and S. Aksela, J. Phys. B **29**, 4387 (1996).
[4] E. v. Raven, M. Meyer, M. Pahler, and B. Sonntag, J. Electron Spectrosc. Relat. Phenom. **52**, 677 (1990).
[5] M. Meyer, E. v. Raven, B. Sonntag, and J. E. Hansen, Phys. Rev. A **43**, 177 (1994).
[6] M. Meyer, E. v. Raven, B. Sonntag, and J. E. Hansen, Phys. Rev. A **49**, 3685 (1991).
[7] T. Hayaishi, Y. Morioka, Y. Kageyama, M. Watanabe, I.H. Suzuki, A. Mikuni, G. Isoyama, S. Asaoka, and M. Nakamura, J. Phys. B **17**, 3511 (1984).
[8] M. Ya. Amusia, M. Yu. Kuchiev, S. A. Sheinerman, and S. I. Scheftel, J. Phys. B **10**, L535 (1977).
[9] A. Niehaus, J. Phys. B **10**, 1845 (1977).
[10] W. Eberhardt, S. Bernstorff, H. W. Jochims, S. B. Whitefield, and B. Craseman, Phys. Rev. A **38**, 3808 (1988).
[11] J. Tulkki, T. Åberg, S. B. Whitefield, and B. Crasemann, Phys. Rev. A **41**, 181 (1990).
[12] G. B. Armen, J. C. Levin, and I. A. Sellin, Phys. Rev. A **53**, 772 (1996).
[13] G. B. Armen and F. P. Larkins, J. Phys. B **24**, 741 (1991).
[14] G. B. Armen and F. P. Larkins, J. Phys. B **25**, 931 (1992).
[15] U. Becker and R. Wehlitz, Phys. Scr. **T41**, 127 (1992).
[16] J. A. R. Samson, W. C. Stolte, Z. X. He, J. N. Cutler, and D. Hansen, Phys. Rev. A **54**, 2099 (1996).
[17] J. A. R. Samson, Y. Lu, and W. Stolte, Phys. Rev. A **56**, R2530 (1997).
[18] P. A. Heimann, D. W. Lindle, T. A. Ferrett, S. H. Liu, L. J. Medhurst, M. N. Piancastelli, D. A. Shirley, U. Becker, H. G. Kerkhoff, B. Langer, D. Szostak, and R. Wehlitz, J. Phys. B **20**, 5005 (1987).

[19] T. Hayaishi, E. Murakami, A. Yagishita, F. Koike, Y. Morioka, and J. E. Hansen, J. Phys. B **21**, 3203 (1988).
[20] L. Avaldi, G. Dawber, R. Camilloni, G. C. King, M. Roper, M. R. F. Siggel, G. Stefani, and M. Zitnik, J. Phys. B **27**, 3953 (1994).
[21] T. D. Thomas, R. I. Hall, M. Hochlaf, H. Kjeldsen, F. Penent, P. Lablanquie, M. Lavollée, and P. Morin, J. Phys. B **29**, 3245 (1996).
[22] H. Kjeldsen, T. D. Thomas, P. Lablanquie, M. Lavollée, F. Penent, M. Hochlaf, and R. I. Hall, J. Phys. B **29**, 1689 (1996).
[23] H. Kossmann, B. Krässig, V. Schmidt, and J. E. Hansen, Phys. Rev. Lett. **58**, 1620 (1987).
[24] S. Svensson, B. Eriksson, N. Martensson, G. Wendin, and U. Gelius, J. Electron Spectrosc. Relat. Phenom. **47**, 327 (1988).
[25] R. I. Hall, L. Alvaldi, G. Dawber, P. M. Rutter, M. A. MacDonald, and G. C. King, J. Phys. B **22**, 3205 (1989).
[26] M. O. Krause, S. B. Whitefield, C. D. Caldwell, J.-Z. Wu, P. van der Meulen, C. A. de Lange, and R. W. C. Hansen, J. Electron Spectrosc. Relat. Phenom. **58**, 79 (1992).
[27] S. Cvejanovic, G. W. Bagley, and T. J. Reddish, J. Phys. B **27**, 5661 (1994).
[28] A. Kikas, S. J. Osborne, A. Ausmees, S. Svensson, O.-P. Sairanen, and S. Aksela, J. Electron Spectrosc. Relat. Phenom. **77**, 241 (1996).
[29] G. C. King, M. Tronc, F. H. Read, and R. C. Bradford, J. Phys. B **10**, 2479 (1977).
[30] C. E. Moore, *Ionization Potentials and Ionization Limits Derived from Optical Spectra*, Natl. Bur. Stan. Ref. Data Ser., Natl. Bur. Stand. (U.S.) Circ. No. 34 (U.S. GPO, Washington, D.C., 1970).
[31] L. Avaldi, R. I. Hall, G. Dawber, P. M. Rutter, and G. C. King, J. Phys. B **24**, 427 (1991).
[32] G. B. Armen and J. C. Levin, Phys. Rev. A **56**, 3734 (1997).